СООБЩЕНИЯ
ОБЪЕДИНЕННОГО
ИНСТИТУТА
ЯДЕРНЫХ
ИССЛЕДОВАНИЙ

Дубна

E9-98-130

O.N.Borisov, N.A.Morozov, E.V.Samsonov, N.G.Shakun,
S.B.Vorojtsov, E.Bakewicz*, H.Doruch*, K.Daniel*,
T.Kwiecien*, R.Taraszkiewicz*

NEW BEAM EXTRACTION SYSTEM FOR THE **AIC-144** CYCLOTRON

*Henryk Niewodniczanski Institute of Nuclear Physics, Krakow, Poland

1998

Performance requirements

The purpose of this study is to propose an efficient beam extraction system for the AIC-144 cyclotron, IFJ, Krakow, Poland[iii]. The following extracted beam properties were assumed

Table 1

Particle	Parameter	Min	Feasible	Max	Option
Proton	Energy (MeV)	20	22.5	60	60.5
	Intensity (μA)	1	–	–	–
Deuteron	Energy (MeV)	20	23.5	30	–
	Intensity (μA)	25	–	–	–
α-particle	Energy (MeV)	–	–	–	max.
	Intensity (μA)	–	–	–	10

The feasibility of the low energy extraction is limited by beam losses on the passage of certain resonances in the tune diagram. An optional requirement, concerning α-particle, implies that the extraction will be performed by a device designed only for proton and deuteron. It was also understood that the intensity requirement will be met if a sufficient internal beam current is accelerated.

Existing extraction system analysis

There are several factors which have precluded the highly efficient particle extraction within the existing system: rather low beam quality due to a large (1.2 mT) amplitude of the first harmonic of the magnetic field at injection, low energy gain per turn ($V_{dee} \leq 50$ kV), limited voltage (≤ 55 kV) at the electrostatic deflector to direct the accelerated particles away from the cyclotron magnetic field. An extraction device similar to the AIC-144 was also operated in the U-120-M cyclotron (Rzez, Czech Republic) and showed a rather low (15 ÷ 20 %) efficiency, i.e. extracted to the internal current ratio[iii].

New extraction system

The layout of the new extraction system is given in Figure 1 and Figure 2. Precession of particle orbit centers, widely used in the extraction of positive ions from compact cyclotrons, has been chosen as a solution of the problem. The precession manifests itself in the fringe magnetic field of the cyclotron due to the well-controlled first harmonic (0.2 ÷ 0.5 mT) of the magnetic field perturbation, which produces radial coherent oscillations of the amplitude (5 ÷ 10) mm. The choice of the precessional extraction method is based on the fact that higher final

energy is reached in a given cyclotron field. It also allows the largest radius, where the ESD (ElectroStatic Deflector) entrance has to be placed. Accordingly, the smallest values of the electric field strength in the ESD could be used.

Computer simulation

The below described procedure was followed in the calculations. In the central region the spatial distribution of the electric field and beam centering were calculated (Figure 3, Figure 4, Figure. 5). In the main acceleration region the magnetic field maps and the corresponding beam transmission were calculated. Near the extraction radius various methods to enhance the orbit separation were considered. The precessional method was chosen as the most suitable for the case. Realistic magnetic field distributions near the extraction radius and along the ejected particle trajectory were interpolated from the measured and calculated maps. The parameters of the deflector and the system for coherent amplitude build up were defined. The magnetic and electrostatic field contribution from the above mentioned devices were included in the main field maps. Various beam deflection simulations were performed in the thus reconstructed fields. We briefly discuss all these steps below.

Magnetic field structure

Prior to the beam dynamics analysis the magnetic field maps for various modes of acceleration should be known. These maps cover both the main acceleration region and the magnet fringe field zone.

Field shaping in the acceleration region (isochronous curves) was performed with the help of the trim coils for protons of 60 MeV (main coil current Io =600 A) and of 22.5 MeV (Io=120 A) and deuterons of 30 MeV (Io=600 A) and of 23.5 MeV (Io=285 A). In the most difficult case (protons of 60 MeV) the accuracy of the mean field shaping was ±1.5 mT at the level of 1.82 T. With the proposed additional valley shims, the deviation of the field from the desired one could be decreased down to ± 0.1 mT.

In the central region the amplitude of the first harmonic was decreased from 1.2 mT down to 0.2÷0.3 mT by means of a better accuracy in manufacturing the central

Turn separation enhancement

The system parameters were chosen mainly to provide extraction of 60 MeV protons because it is the most difficult case for the extraction process.

A set of particles with the initial radial amplitudes of 0, 1, 2, 3, 4 and 5 mm, (emittance = 37 π×mm×mrad), axial amplitudes of 1, 2 and 3 mm (emittance = 4.5 π×mm×mrad), energy of 55 MeV, belonging to the beam bunch of (–30°)÷(–10°) RF width, were traced through the extraction region. This rather good beam quality could be taken for the calculations as a result of the first magnetic

field harmonic suppression in the central region and the centering and beam transmission studies.

Due to passing the $2Q_z=Q_r$ coupling resonance, with Q_r and Q_z the radial and axial oscillation frequencies (Figure. 6),the axial amplitudes of some particles increase and the extracted beam axial emittance goes up to 12 π×mm×mrad (Figure. 9). The optimal values of the first harmonic amplitude (0.2 mT) and its phase (170°) were obtained to provide ≈ 3.6 mm radial turn separation at the ESD mouth (azimuth 98°). The ESD entrance position should be at the radius 62.9 cm to reduce the radial beam losses at its septum down to 10 ÷ 15 %, provided the septum width is 0.5 mm (Figure. 7). The radial emittance of the beam equals 11 π×mm×mrad and the energy is 60.08 ± 0.17 MeV there (Figure. 8).

When simulating the extracting process of 22.5 MeV protons, the procedure similar to protons of 60 MeV was employed. Here, the main difference is the higher maximal separation between two successive turns (≈ 11 mm). Of course, the following parameters of the extraction system should be adjusted as required: V_{dee}, the first harmonic amplitude and its phase, ESD entrance position and aperture. But these values are less demanding than in the previous case. The same is valid for deuterons and α-particles within their specified energy range.

A new system of harmonic coils is proposed to produce the required magnetic field perturbation. (Figure. 14) It will be placed near the surface of the valley shims, in the radial range 61÷68 cm. Having 400A×4turns in one coil, one could expect the amplitude of the first harmonic ≈ 1.2 mT with any desired phase.

Beam deflection

Again, the basic parameters were chosen for the extraction of 60 MeV protons. The existing system constraints should be obeyed too. Three electrostatic deflector sections and three magnetic channel sections are used (Figure. 10, Figure. 11) for the beam deflection to the matching point with the cylindrical coordinates R = 153 cm and azimuth = 308°, the desired beam spot dimensions being 10×10 mm there (Figure. 12, Figure. 13). The corresponding radial and axial envelopes were also calculated.

Deflection of 22.5 MeV protons, deuterons and α-particles within the specified energy ranges requires a suitable adjustment of the parameters of all the deflector sections. But, again, their values are less demanding than in the case with 60 MeV protons. It was also understood that the extraction of particles of any intermediate energy (in between the above considered extremities) could be easily provided by the proposed device.

As an example, some parameters of the deflector for the case of 60 MeV protons are summarized in Table 2.

The ESD-1 section (Figure. 15, Figure. 16) allows one to use lower voltage in the ESD to provide required beam deflection at the MC-1 (Magnetic Channel)

section mouth. The preliminary design of the ESD sections was made with the help of the well known ELCUT (QuickField) code. In order to reduce the cyclotron magnetic field along the extraction paths and to provide horizontal focusing for compensating for the defocusing effect of the cyclotron fringe field, passive magnetic channel sections MC-1 (Figure. 17) and MC-2 are employed. A relatively low magnet field (≤ 0.3 T) near the MC-3 section allows its active design (Figure. 18). The radial gradients of the sections are adjusted by changing ampere turns in the coil (400A × 3 turns / pole).

Conclusion

A new extraction system for the cyclotron AIC-144 is proposed. Computer simulation shows its potentially high efficiency for the specified set of particles and range of their energies.

Table 2

Parameter	ESD-1	ESD-2	ESD-3	MC-1	MC-2	MC-3
Θ_{ent} (deg)	98	120	140	183	215	273
Θ_{exit} (deg)	112	140	177	205	250	283
R_{ent}(cm)	62.9	62.9	64.0	65.8	67.8	89.8
R_{exit} (cm)	62.7	64.0	65.7	66.8	76.2	99.9
V (kV)	55	55	55	-	-	-
E (kV/cm)	120.7	120.7	100.9	-	-	-
B (T)	-	-	-	-0.183	-0.223	0
dE/dR (kV/cm^2)	0	0	-46.1	-	-	-
dB/dR (T/)	-	-	-	0	8	12
$dX \times dZ_{ent}$ (mm^2)	4.5 x 10	4.5 x 10	4.5 x 10	8 x 10	12 x 10	20 x 10
$dX \times dZ_{exit}$ (mm^2)	"---"	"--"	7 x 10	"--"	"--"	"--"

The authors would like to express their gratitude to O.V.Lomakina and A.S.Galoyan for their help in preparing this manuscript.

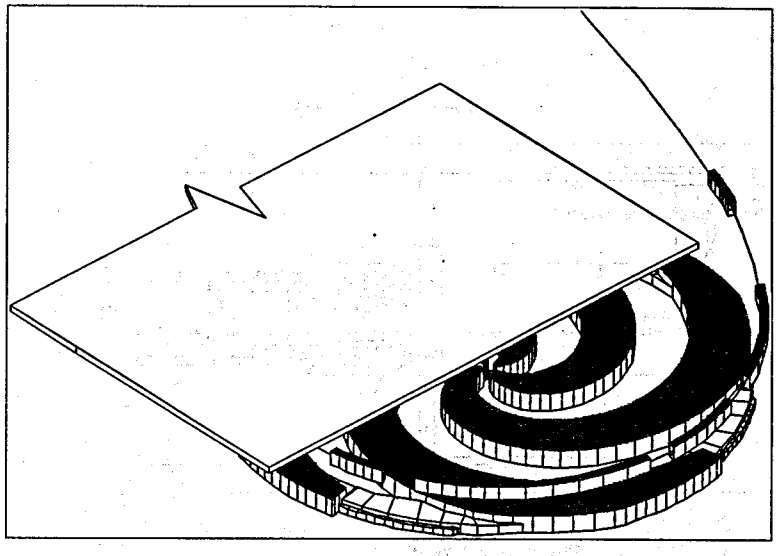

Figure 1 Magnetic structure of the AIC-144 cyclotron with the extraction system shown

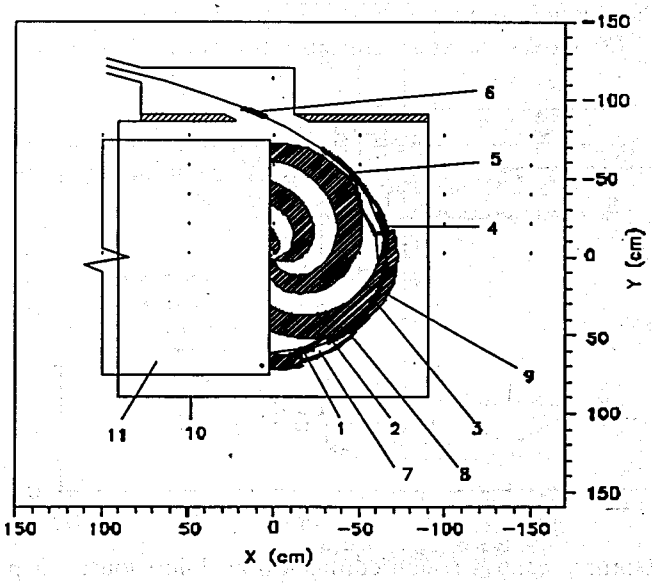

Figure 2 Extraction system layout. 1,2,3-electrostatic deflector sections ESD-1,2,3; 4,5,6-magnetic chanel sections MC-1,2,3; 7-valley shim; 8-harmonic coil; 9-spiral shim; 10-vacuum chamber; 11-dee

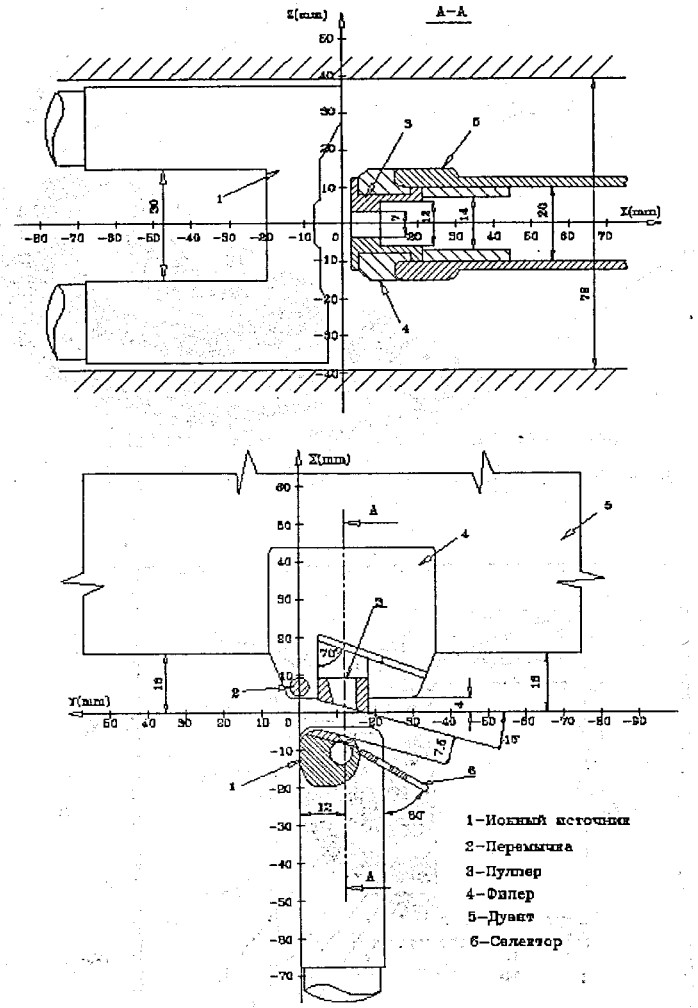

Figure 3 Optimal central region configuration. 1-ion source; 3-puller; 4-feeler; 5-dee, 6-selector

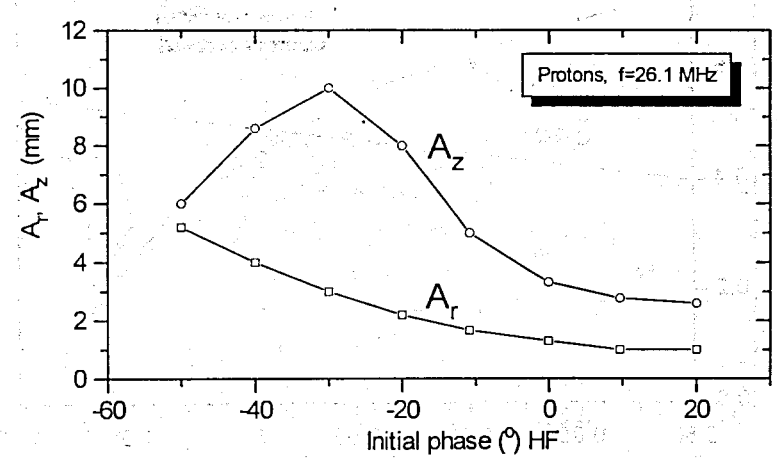

Figure 4 Radial amplitudes after 20 turns and axial amplitudes during the initial 5 turns (their starting values Z_o=2mm, Z_o'=0)

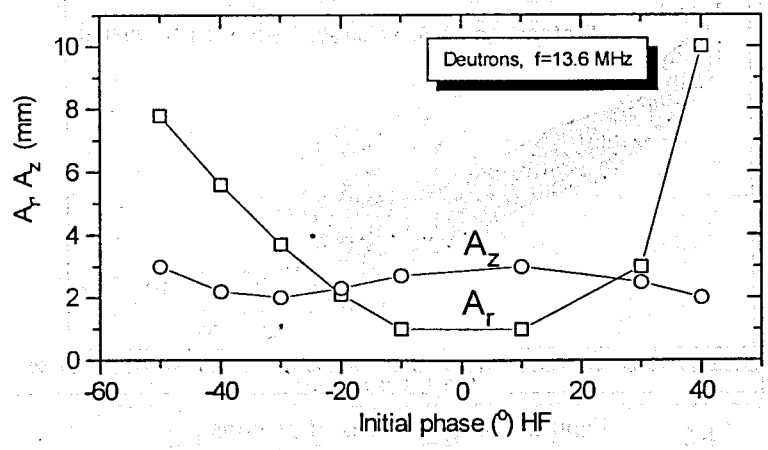

Figure. 5 Radial amplitudes after 15 turns and axial amplitudes during the initial 5 turns (their starting values Z_o=2mm, Z_o'=0)

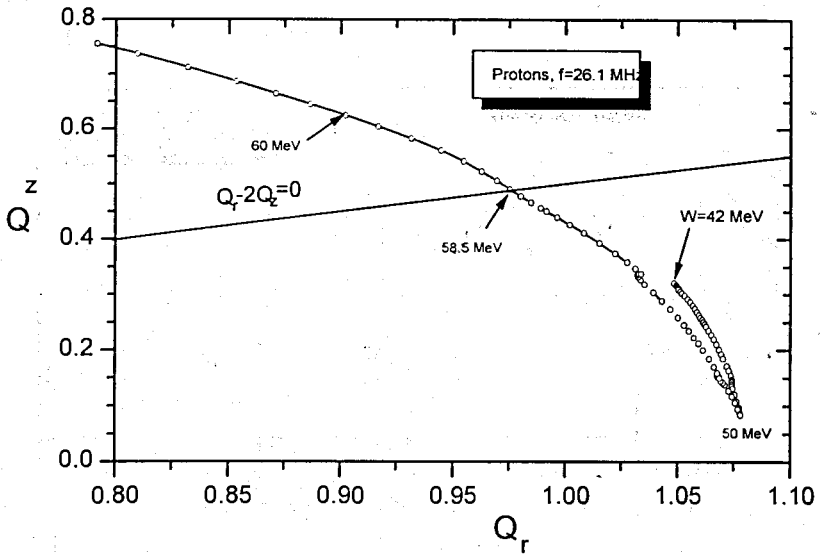

Figure. 6 Betatron frequencies for protons of 60 MeV

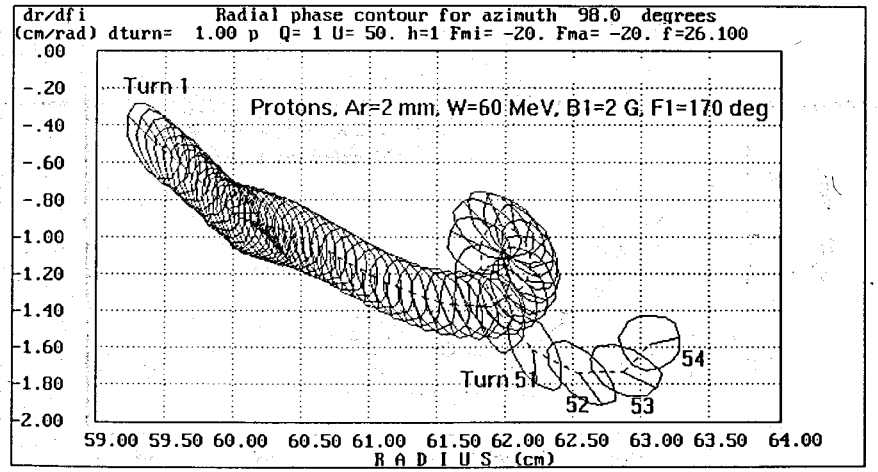

Figure. 7 Last 54 turns of protons

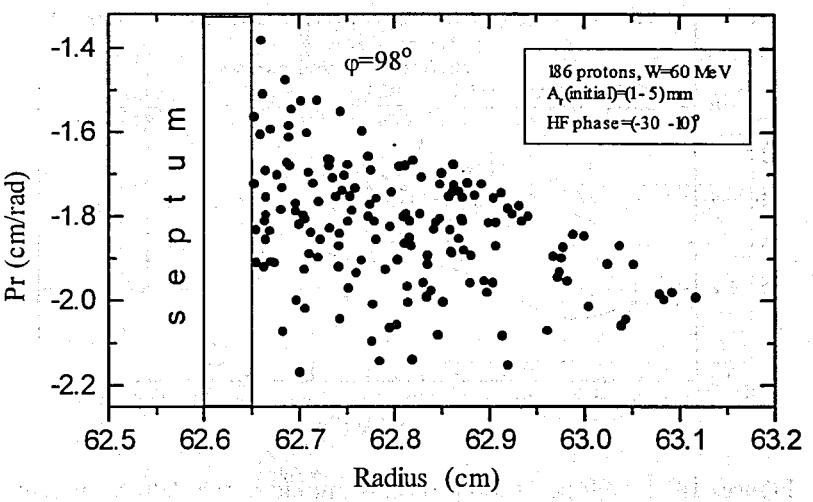

Figure. 8 Radial emittance of protons at the mouth of the ESD

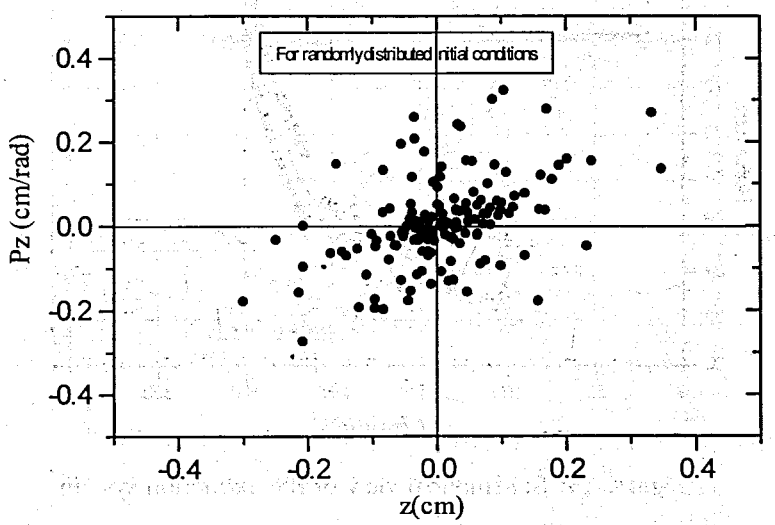

Figure. 9 Axial emittance of protons at the mouth of the ESD

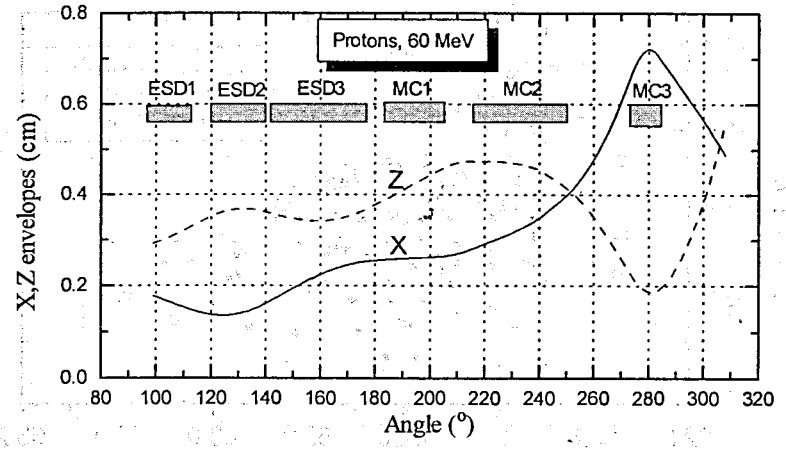

Figure. 10 Envelope of the proton beam along the deflection system

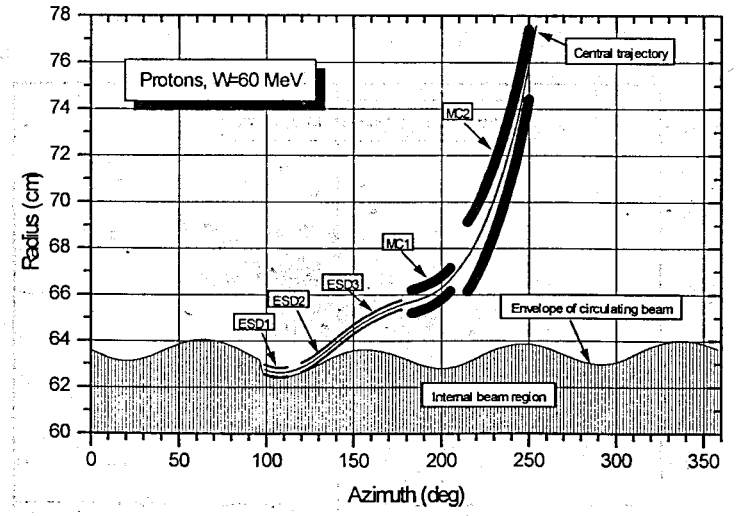

Figure. 11 Schematical view of the extraction system

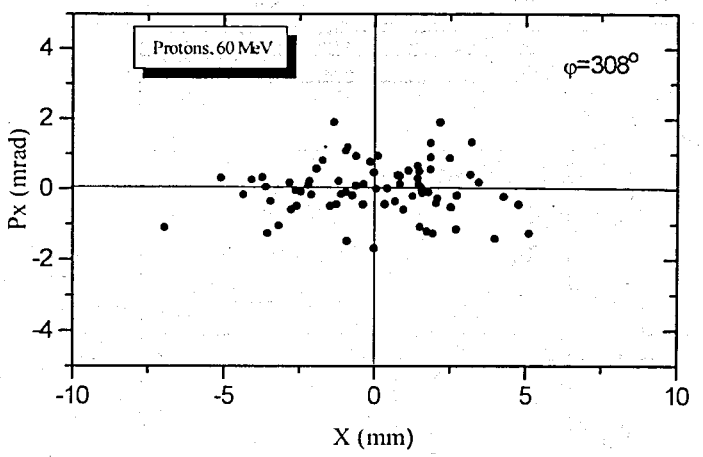

Figure. 12 Radial emittance of the extracted proton beam

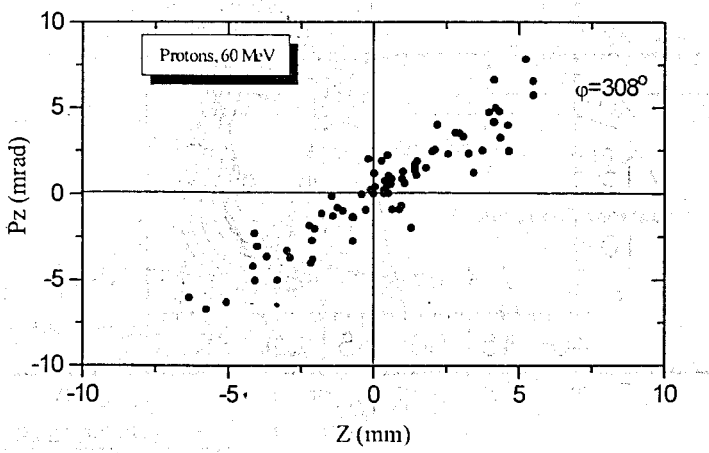

Figure. 13 Axial emittance of the extracted proton beam

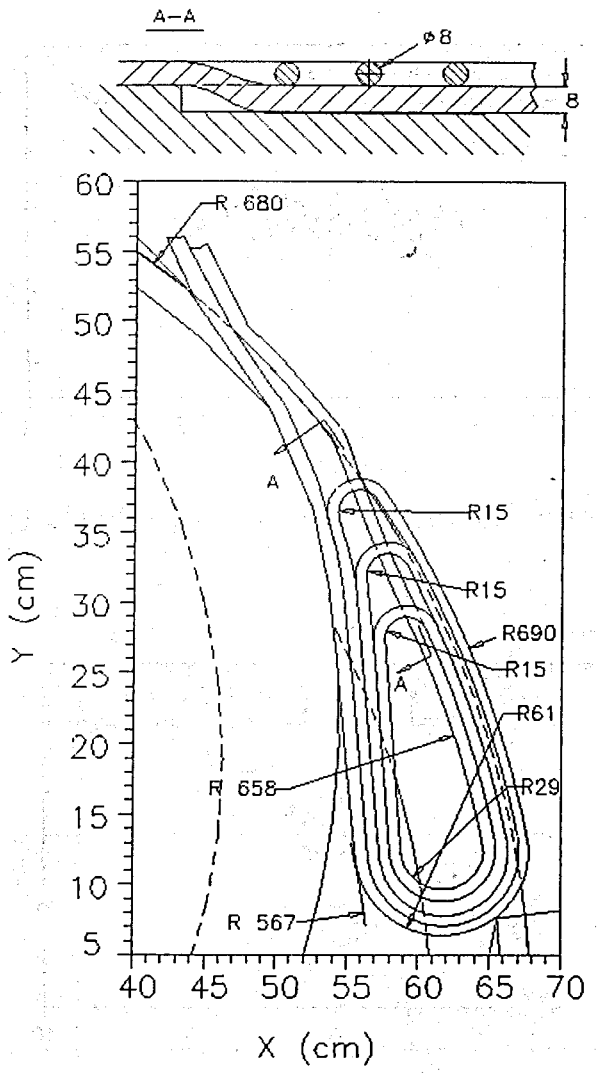

Figure. 14 Harmonic coil layout

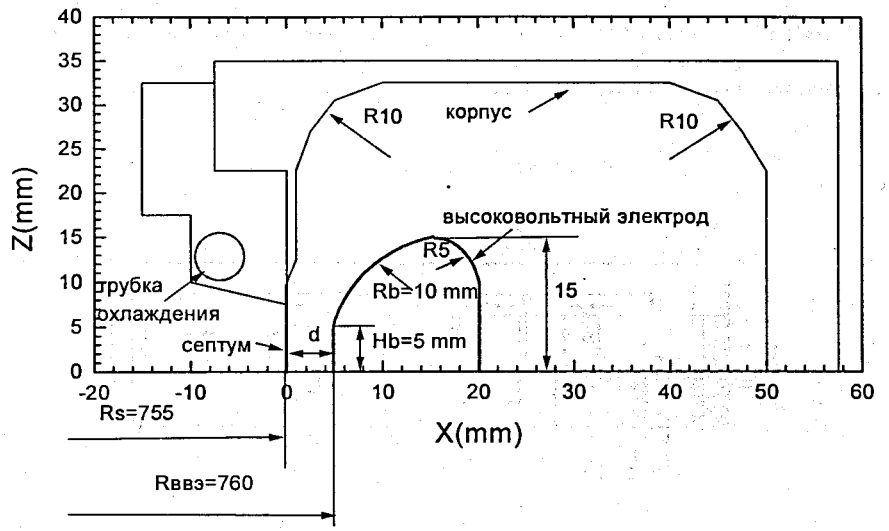

Figure. 15 ESD-1 cross section

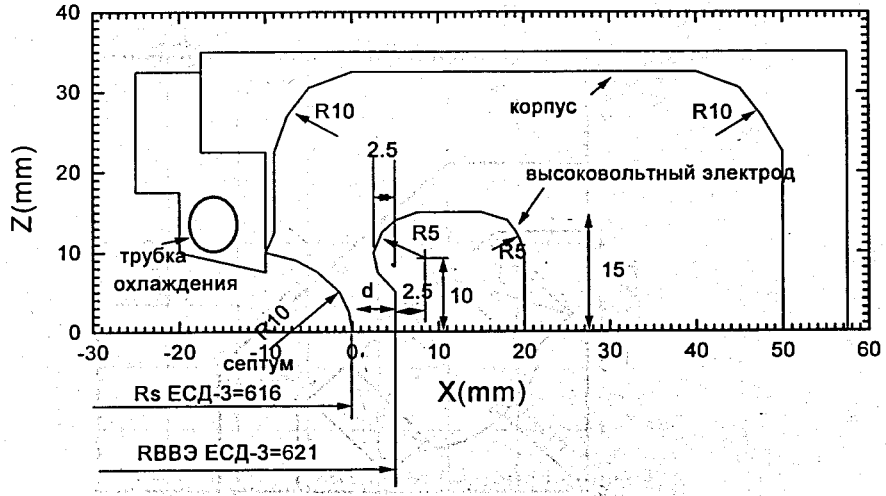

Figure. 16 ESD-3 cross section

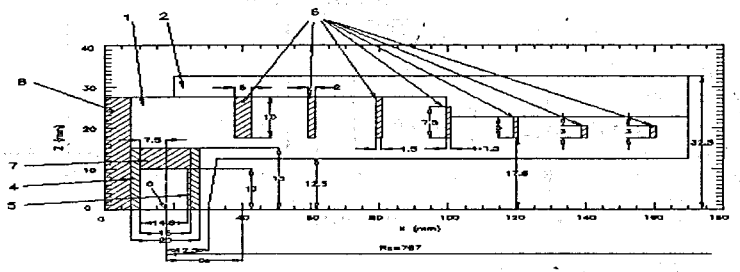

Figure. 17 MC-1 cross section. 1- Al case, 2 - cap-1, 4,5 - main Fe shims, 6 - trim Fe shims, 7 - plate, 8 - cap-2.

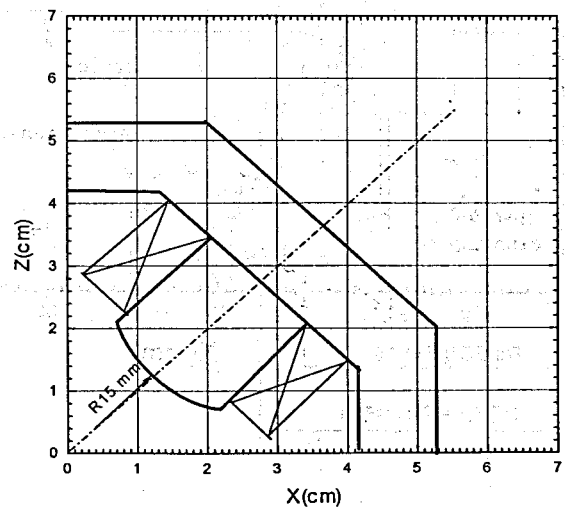

Figure. 18 MC-3 cross section.

References

[ii] J.Schwabe, J.Starzewski, A.Semkowicz, V.P.Dmitrievski, A.A.Glazov, V.V.Kolga, N.L.Zaplatin. "Automatic Isochronous Cyclotron AIC-144". In: Proceedings of the International Seminar on Isochronous Cyclotron Technique. Krakow, Poland, November 13 - 18, 1978, p.197, IFJ Report N 1069/PL.

[iii] Z.Trejbal, Communications of the JINR 9-10388, Dubna, 1977.

Received by Publishing Department
on May 15, 1998.